

Calculated evolution of the Electron Bernstein Wave heating deposition profile under NBI conditions in TJ-II plasmas

A. Cappa¹, D. López-Bruna¹, F. Castejón¹, M. Ochando¹

J. L. Vázquez-Poletti², M. Tereshchenko³, E. Huedo² and I.M. Llorente²

¹ *Laboratorio Nacional de Fusión, Madrid, Spain*

² *Facultad de Informática, Universidad Complutense de Madrid, Madrid, Spain*

³ *Instituto de Biocomputación y Física de Sistemas Complejos, Zaragoza, Spain*

Introduction

A system for EBW heating in the TJ-II stellarator will start operation in the second half of 2009. This system is intended to be used routinely for heating at high densities, well over the O and X modes cutoff.

Ray tracing calculations of the O-X-B mode conversion at first harmonic ($f = 28$ GHz) have shown the feasibility of this heating scenario in TJ-II under different –but fixed– densities and temperatures [1]. From these calculations, it is clear that the properties of the O-X-B heating depend strongly on the density and temperature profiles.

The central densities that are needed to have the first harmonic O mode cutoff located at the plasma periphery, where the O-X mode conversion occurs, are achieved either by an external gas puffing or by NBI fuelling in NBI discharges. On the other hand, the resultant density ramp-up makes appear the cutoff density of the second harmonic X mode ($n_c = 1.75 \times 10^{19}$ for $f = 53.2$ GHz) and, because of this, the ECRH heating efficiency vanishes. Therefore, a smooth transition between ECRH and EBW+NBI heated plasmas –in which the radiative collapse should be avoided– is not guaranteed and a time dependent transport calculation that can take into account the evolution of the EBW power deposition profile may help us to understand such a transition and find the experimental settings for an optimum operation in this regime. Moreover, the conditions in which a radiative collapse in NBI plasmas is reached depends not only on the added heating power, but also on the shape of the power deposition profile itself [2].

Time dependent calculations: TRUBA & ASTRA

A self-consistent transport calculation require a large CPU time since it is necessary to evaluate the EBW power deposition profile as the density and the temperature profiles evolve. Besides, to obtain an accurate calculation of the power deposition profile, a large number of rays (193 are considered here) must be used to simulate the incident microwave beam. Recent developments of grid computing [3] have allowed extensive ray tracing calculations in the TJ-II

Heliac geometry using the TRUBA code [4]. To obtain the plasma parameters evolution we include transport and impurity radiation models in the ASTRA (Automated System for Transport Analysis) framework [5] with the underlying assumption that the heating method does not change the nature of transport in the plasma regimes under study. Therefore, any transport coefficients that reproduce the evolution of TJ-II plasma profiles in the relevant conditions are valid for our purpose and their details are not critical. On the other hand, the sources terms have been calculated with care giving special importance to the radiation term. Particle source terms in agreement with the experimental data [6] have been obtained using an adaptation of the Eirene code and the NBI power deposition has been estimated with the Fafner II code.

Results

We have taken TJ-II discharge #14931 as a model case for comparison. The simulation

starts with stationary $n_e(\rho)$, $T_e(\rho)$, $\bar{n}_e \approx 0.6 - 0.7 \times 10^{19} \text{ m}^{-3}$ and $T_e(\rho = 0) \approx 1 \text{ keV}$. A very important parameter in these simulations is the effective charge, Z_{eff} , whose maximum here is set to $Z_{\text{eff}} = 1.85$ (ECRH phase). The shot represented in Fig. 1 (top) collapses because, after the ECRH cutoff density is reached, the plasma temperature drops to values where the cooling rates increase the lower the temperature, which is the situation that provokes a radiative instability. If the densities are not high enough for the NBI deposition to be efficient, the radiated power can easily surpass the heating power, thus quenching the plasma. The addition of EBW heating power clearly helps in prolonging the discharge (Fig. 1 (bottom)). From the beginning, the efficiency of the EBW heating is very high. Shortly after the appearance of the O-mode cutoff, essentially all the EBW power is absorbed. Since this happens before the ECRH cutoff density is reached, there is some time of overlapping of the two electron heat sources and the calculations predict no plasma collapse in the transition between heating schemes, even if the NBI heating is still ineffective due

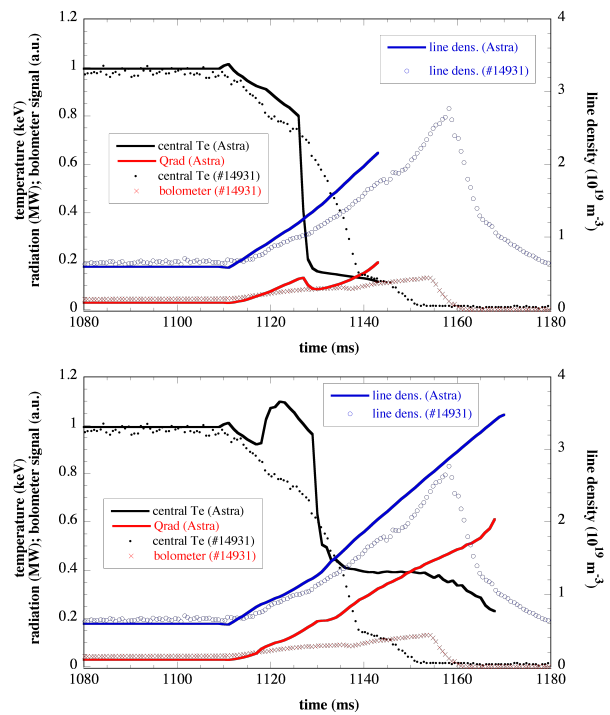


Figure 1: *Experimental traces from a collapsing NBI discharge without (top) and with (bottom) EBW heating. The result of the numerical simulation is shown with solid lines. In both cases, the simulation ends when the temperature drops to zero due to a radiative collapse.*

to the low density. Note that the radiated power is larger during the phase of overlapping of the three heating methods (see Fig. 2). However, in the case without EBW and when the ECRH heating stops, the total power balance to the electrons becomes negative for a few milliseconds due to the poor NBI heating efficiency. This causes a rapid electron temperature drop. With EBW this momentary negative power balance is avoided and large radiated powers can be sustained for a longer time without the plasma undergoing a radiative collapse. The evolution of the electron temperature and density profiles is shown in Fig. 3. During the transition from ECRH to EBW, there is sharp drop in the central temperature while the density keeps on growing.

The shape of these profiles changes drastically when the EBW+NBI phase is entered: the plasma starts with peaked temperature profile and hollow density one, as it corresponds to the usual features of ECRH heated plasmas in TJ-II, and evolves towards much flatter profiles. Thomson Scattering data taken at different densities on similar NBI discharges –although, obviously, without EBW heating– show such features systematically. The added EBW heating changes slightly the T_e profile at these heating powers.

Finally, the evolution of the EBW power deposition profile is shown in Fig. 4. At $t \approx 1120$ ms, the maximum of the absorption happens at $\rho = 0.7$. Then, this peak is reduced and moves inwards, and a centred peak of absorption appears as the density increases. For $t > 1140$ ms (correspond-

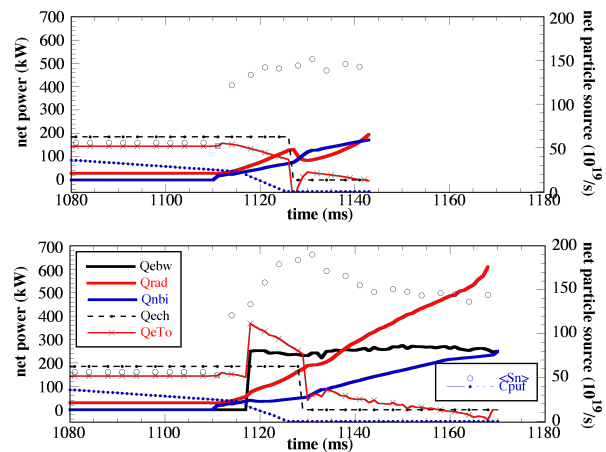


Figure 2: Net power balance without (top) and with EBW heating (bottom).

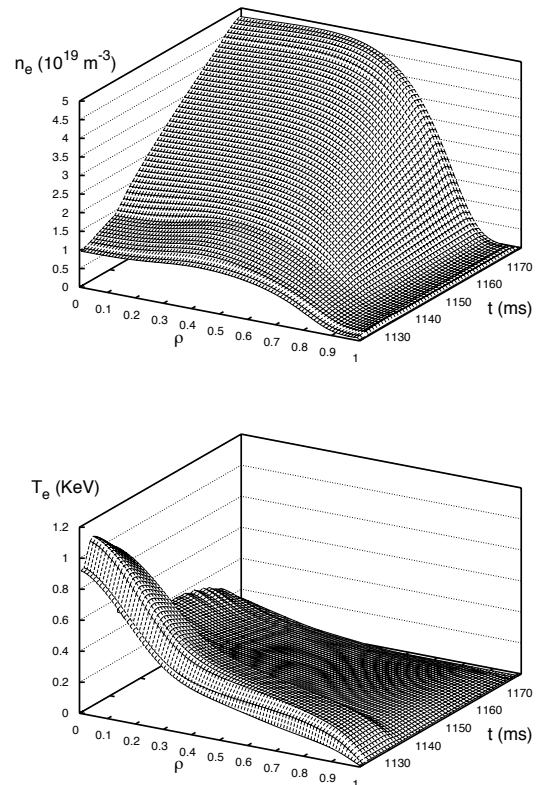


Figure 3: Time evolution of the electron density (top) and temperature (bottom) profiles.

ing to central densities $n_e(\rho = 0) \gtrsim 2 \times 10^{19} \text{ m}^{-3}$, the power deposition profile does not change substantially and exhibits a maximum close the plasma centre, with a power density of about 5 W/cm^3 and a second peak with power densities of 1 W/cm^3 . The simulations show that the collapse of the NBI discharge is retarded with the help of EBW, not because the added EBW power deposition profile heats the edge plasma region, where the intense electron heat losses through radiation start, but due to a favourable net power balance to the electrons. Nevertheless, these calculations indicate that the self-consistent evolution of the deposition profile is necessary to study different plasma scenarios.

Conclusions

The ray tracing code TRUBA has been connected to the ASTRA system in order to investigate the transit from ECRH to EBW+NBI heated plasmas. The large number of rays used in the simulation of the EBW power deposition profile (193 rays 50 times) have been calculated using grid computing techniques. Radiation losses have been taken into account in the simulation. According to the calculations, radiative collapse does not occur during the transition and its appearance is avoided if EBW heating is added. The need for self-consistent calculations has been underlined.

References

- [1] F. Castejón *et al*, Nucl. Fusion **48** 075011 (2008)
- [2] M. A. Ochando *et al*, Nucl. Fusion **37** 225 (1997)
- [3] J. L. Vázquez-Poletti *et al*, Multiagent and Grid Systems **3**, n. 4, 429 (2007)
- [4] M. A. Tereshchenko *et al*, 30th EPS Conference on Contr. Fusion and Plasma Phys. ECA **27A** P-1.18 (2003)
- [5] G.V. Pereverzev, P.N. Yushmanov, *Astra: Automated System for Transport Analysis*, IPP **5/98**, Garching, February 2002
- [6] V. I. Vargas *et al*, Informes Técnicos CIEMAT **1162**, February 2009

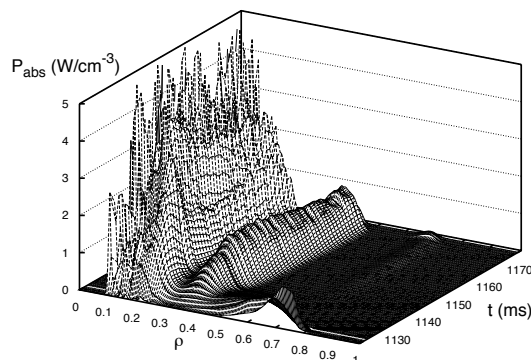


Figure 4: Time evolution of the EBW power deposition profile obtained from ray tracing.